

Optimized NGFR-derived hinges for rapid and efficient enrichment and detection of CAR T cells *in vitro* and *in vivo*

A. Bister,^{1,2} T. Ibach,² C. Haist,^{1,2} G. Gerhorst,² D. Smorra,¹ M. Soldierer,¹ K. Roellecke,² M. Wagenmann,² K. Scheckenbach,² N. Gattermann,³ C. Wiek,^{2,4} and H. Hanenberg^{1,2,4}

¹Department of Pediatrics III, University Children's Hospital, University of Duisburg-Essen, Hufelandstr. 55, 45122 Essen, Germany; ²Department of Otorhinolaryngology, Head & Neck Surgery, Heinrich Heine University, Düsseldorf, Germany; ³Department of Hematology, Heinrich Heine University, Düsseldorf, Germany

Chimeric antigen receptor (CAR) T cell therapy has demonstrated unprecedented success with high remission rates for heavily pretreated patients with hematological malignancies. The hinge connecting the extracellular antigen recognition unit to the transmembrane domain provides the length and flexibility of the CAR constructs and ensures that the CAR can reach the target antigen and mediate recognition and killing of target cells. The hinge can also include specific amino acid sequences to improve CAR expression, influence T cell proliferation, and facilitate CAR T cell detection, enrichment, and even elimination. Here, we report the generation of two novel hinge domains derived from the low-affinity p75 chain of the human nerve growth factor receptor (NGFR), termed N3 and N4, which, when incorporated into the CAR backbone, allow detection as well as high-grade enrichment of CAR T cells with GMP-compatible immunomagnetic reagents. After optimizing the MACS protocol for excellent CAR T cell purity and yield, we demonstrated that N3- and N4-hinged CAR T cells are as efficacious as their CD8-hinged counterparts *in vitro* against hematological blasts and also *in vivo* in the control of acute monocytic leukemia in an immunodeficient mouse xenograft model. Thus, both hinges could potentially be an integral part of future CAR designs and universally applicable in clinical applications.

INTRODUCTION

More than three decades after the first concept studies,¹ the amazing clinical success of chimeric antigen receptor (CAR) T cell therapy in the last couple of years has transformed the clinical care of patients with poor-prognosis hematological malignancies.² For clinical CAR T cell therapy, autologous T cells from patients with leukemia and lymphoma are transduced *in vitro* with lentivirally expressed CAR constructs that typically combine the antigen recognition ability of monoclonal antibodies in *cis* with functional domains of T cell receptor signaling, including epitope recognition, activation, and expansion, in a single molecule.² Currently, six different CAR products have received market approval for hematological malignancies, namely Kymriah, Yescarta, Tecartus, and Breyanzi for CD19-positive

leukemias or lymphomas, and Abecma and Carvykti for BCMA-positive multiple myelomas.^{3,4}

The second-generation CAR constructs used in these six formulations contain single-chain variable fragments (scFvs) of monoclonal antibodies linked in *cis* via a hinge/spacer and a transmembrane region to the intracellular signaling domains of the CD3 ζ -chain and the co-stimulatory receptors CD28 or 4-1BB/CD137.^{2,3} Importantly, the design of this single chimeric protein ensures that the CAR molecules mediate MHC-independent T cell activation and killing of malignant as well as normal cells if the target antigen is expressed.^{2,3} Although the hinge can theoretically influence the function of CAR constructs, only few candidates for this domain in CARs have been thoroughly investigated.^{3,5–18} One key aspect to consider for the length and flexibility of a hinge is the location of the epitope recognized by the CAR scFvs within the three-dimensional structure of the target antigen.^{5,13} In addition, incorporating a specific hinge can improve the protein expression and stability of the CAR and can modulate the expansion, proliferation, and stimulation of the CAR T cells.^{9,10,14,18} Most clinically used CARs contain hinges derived from human CD8 or CD28, which appear to be safe to use as they are naturally expressed on T cells and by themselves do not confer additional features to the CAR T cells.^{19–22} However, instead of using the hinge as neutral element that simply connects the scFvs to the transmembrane and signaling domains, endeavors have been made to modulate the hinge for improvement of T cell stimulation (patent EP3184548A1) for *in vivo* detection and/or elimination of CAR T cells^{15,23} and for enrichment of transduced T cells *in vitro* before infusion into patients.^{12,23,24}

Received 8 February 2022; accepted 27 May 2022;
<https://doi.org/10.1016/j.omto.2022.05.012>.

⁴These authors contributed equally

Correspondence: Helmut Hanenberg, Department of Pediatrics III, University Children's Hospital, University of Duisburg-Essen, Hufelandstr. 55, 45122 Essen, MD, Essen, Germany.

E-mail: Helmut.Hanenberg@uk-essen.de



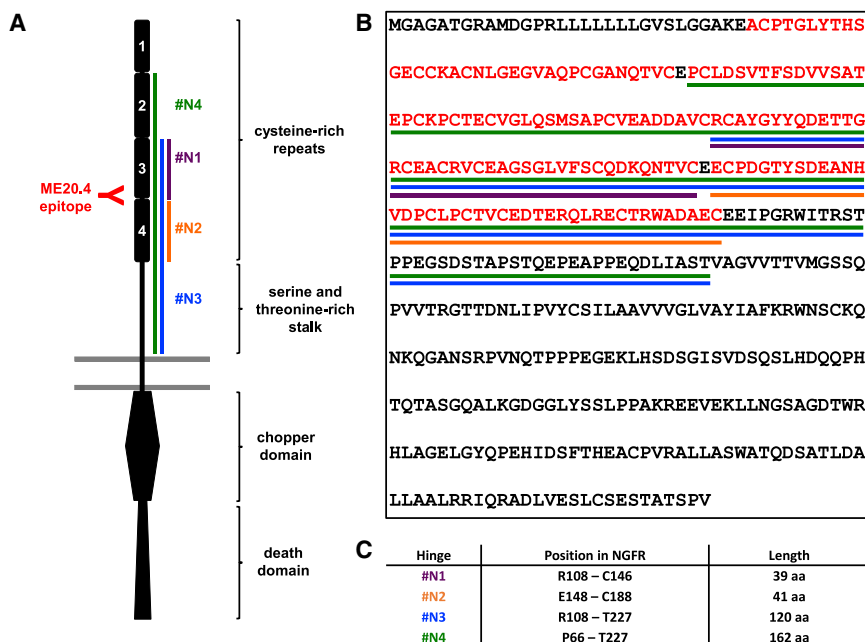


Figure 1. Structure and amino acid sequence of NGFR- and NGFR-derived hinges

(A) NGFR consists extracellularly of four cysteine-rich domains (CRDs) and a serine/threonine-rich (S/T)-rich stalk. Intracellularly, it carries a chopper and a death domain. The NGFR antibody (clone ME20.4) presumably binds an epitope in the third and/or fourth cysteine-rich repeat. The novel NGFR-derived hinges consist of the third CRD (N1, 39 aa), the fourth CRD (N2, 41 aa), the third and fourth CRD plus the stalk (N3, 120 aa), or the second, third, and fourth CRD plus the stalk (N4, 162 aa). (B) The amino acid sequences of the hinges are indicated in the NGFR amino acid sequence by lines in the corresponding color. The CRDs are shown in red. (C) Tabular overview of the NGFR-derived hinges, their length and position within NGFR.

Several methods to quantify CAR T cell persistence in patients exist: Idiotypic antibodies^{25,26} and tagged antigens^{27,28} bind the CAR construct directly and thus allow to precisely visualize the CAR expression on protein level; however, both detection reagents have to be adapted whenever a new antigen is targeted.²⁵ CAR T cell persistence can also be measured on the mRNA level by qRT-PCR,^{31–33} ddPCR,²⁷ or RNA-sequencing;³⁴ however, this analysis will not address protein translation or stability issues. Cell surface markers^{29,30} can be co-expressed with CAR constructs in the same vector, however this approach will increase vector size, thus influencing transduction efficiency³⁵, and both transgenes will not necessarily be expressed at similar ratios.³⁶ Ultimately, as flow cytometric methods will allow to specifically assess the CAR T cell phenotype, including activation and exhaustion markers,^{7,12} the inclusion of an epitope recognizable by antibodies into the hinge of CARs combines the advantages of all these strategies.

The extracellular sequence of nerve growth factor receptor (NGFR) contains a 28 amino acid (aa) leader peptide, four cysteine-rich domains (CRDs) of approximately 40 aa each and a serine/threonine (S/T)-rich stalk followed by a single-pass transmembrane domain.³⁷ For more than 30 years, this structure, with and also without the 155 aa cytoplasmic tail, has been used as a marker for successful gene transfer in research as well as clinical settings.^{38–40} In 2002, the description of insertional mutagenesis in a murine transplantation model with a splice-active oncoretroviral vector, where the cytoplasmically truncated NGFR (Δ NGFR) was expressed off the strong 5' LTR, questioned the safety of using the Δ NGFR cDNA as transgene for human clinical applications.⁴¹ However, Bonini et al.⁴² reported the successful transduction of more than 7×10^9 bone marrow cells with subsequent infusion into over 900 mice, rats and dogs without a

single oncogenic transformation and Ciceri et al.³⁸ used the Δ NGFR as a magnetic cell sorting (MACS) selection marker for suicide gene-expressing allogeneic T cells in clinical studies without any insertional mutagenesis. In 2018, Casucci et al.¹² systematically investigated the potential of the Δ NGFR as a hinge for CAR T cells, testing different lengths of the extracellular sequences in lentiviral CAR expression constructs. Although detection of the CAR construct on transduced T cells was readily possible with an NGFR antibody, the authors could not efficiently enrich Δ NGFR-hinged CAR T cells with directly coupled LNGFR/CD271 microbeads.¹² In a follow-up study, the same group further improved the hinge regarding cytotoxicity by including additional amino acids from the stalk, but still failed to efficiently enrich their NGFR-hinged CAR T cells with GMP-compatible microbeads.¹⁷

Here, we describe the successful establishment of two novel NGFR-derived hinges termed N3 and N4, which mediate efficient selection of CAR T cells against hematological cancers and are functionally indistinguishable from a clinically well-established human CD8-derived hinge^{12,17} *in vitro* and *in vivo* in immunodeficient mice.

RESULTS

Design of NGFR-derived hinges for CARs

The NGFR antibody clone ME20.4 used by Miltenyi Biotec in their NGFR microbeads for MACS selection binds an epitope in the third and/or fourth CRD in the extracellular part of NGFR (personal communication with Miltenyi Biotec 2015).¹² Therefore, we designed four new NGFR sequences around the third and fourth CRD to be included as hinges into our CAR constructs (Figure 1): The two short hinges N1 (39 aa) and N2 (41 aa) only consisted of the third or fourth CRD, respectively. N3 (120 aa) contained the third and fourth CRD plus the S/T-rich stalk and N4 (162 aa) additionally the second CRD. For control constructs (described below), we used the complete codon-optimized surface and transmembrane regions of NGFR, but deleted the cytoplasmic chopper and death domains (Figure 1).

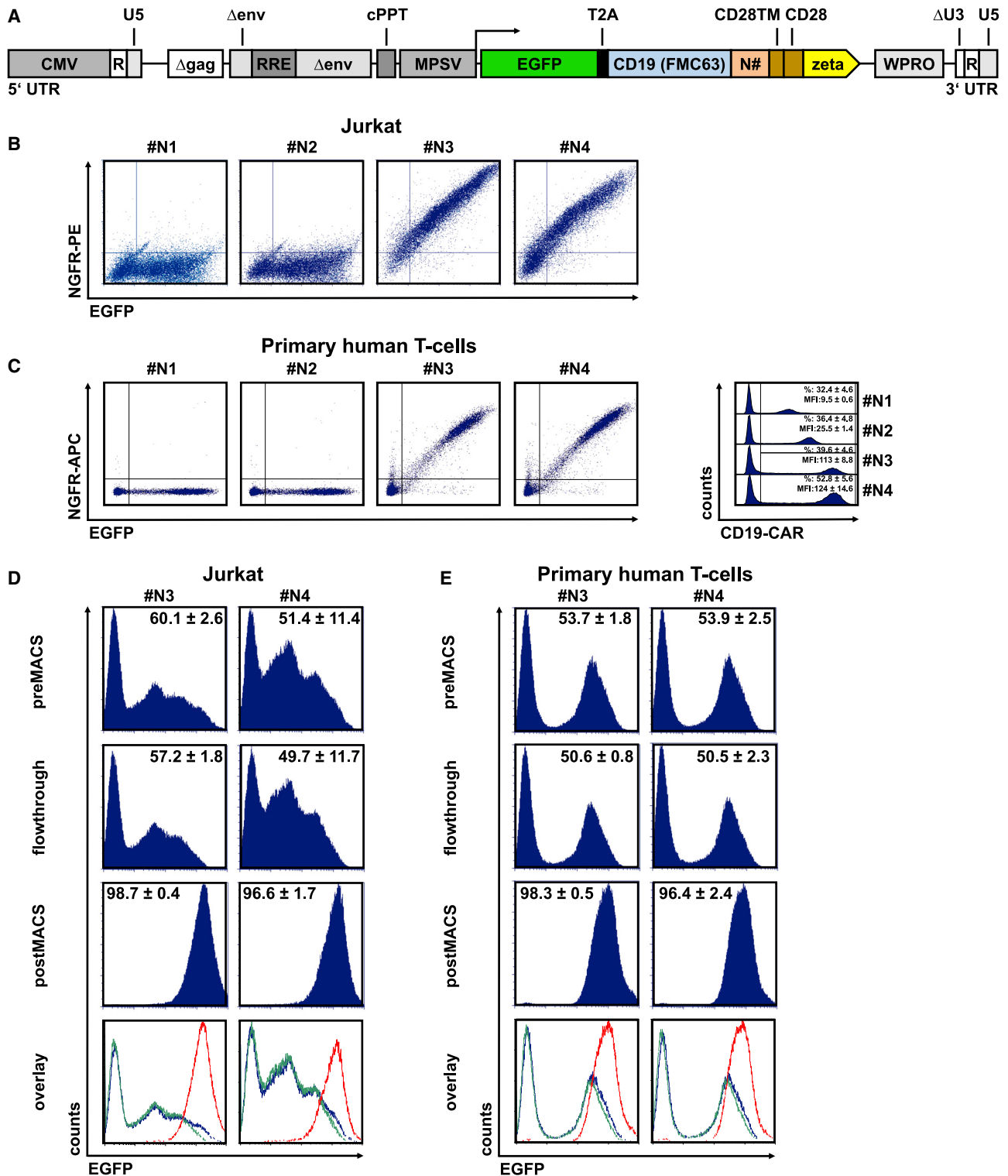


Figure 2. Expression and enrichment of NGFR-hinged CARs in Jurkat and primary human T cells

Jurkat or primary human T cells were lentivirally transduced with constructs co-expressing EGFP in *cis* with N1-, N2-, N3-, or N4-hinged CD19 CARs depicted in (A). Three days after transduction Jurkat cells (B) or primary human T cells (C) were flow cytometrically analyzed for their CAR expression levels (via staining with NGFR-PE, clone

(legend continued on next page)

NGFR-hinged CAR expression and enrichment on MACS MS columns

The fragments N1-N4 were inserted into a previously published human codon-optimized CD19 CAR construct in a bicistronic lentiviral vector (Figure 2A), thereby replacing the 229 aa IgG1-derived CH₂CH₃ hinge.⁴³ To test whether the CARs with the four NGFR hinges are stably expressed on the surface of transduced cells and bind the ME20.4 NGFR antibody, we transduced Jurkat and primary human T cells with VSV-G-pseudotyped bicistronic lentiviral vectors co-expressing EGFP and N1-N4-hinged CD19 CARs (Figure 2A). After 5 days, the transduced cells were stained with ME20.4-PE and then analyzed for NGFR as well as EGFP expression by flow cytometry. Although the EGFP expression in Jurkat (Figure 2B) and primary human T cells (Figure 2C) was comparable for all four constructs, only N3- and N4-hinged CD19 CARs showed a clear co-expression of NGFR and EGFP (Figures 2B and 2C). We also co-stained the CAR T cells with the CD19 CAR detection reagent developed by Miltenyi Biotec. While both the N1- as well as the N2-hinged CD19 CAR bound the CD19 CAR detection reagent and thus the CARs were indeed expressed on the surface of the T cells, the expression levels were much lower compared to the N3- and N4-hinged constructs (Figure 2C), demonstrating that the NGFR monoclonal antibody cannot bind N1- and N2-hinged CARs and suggesting that the N1 and N2 constructs were less stable. Since N1 and N2 could not be used for detection or selection of CAR T cells, these hinges were not included in further experiments.

Next, we transduced Jurkat and primary human T cells with VSV-G pseudotyped lentiviral particles introducing the N3- and N4-hinged CD19 CAR bicistronic vectors (Figure 2A) and then used *Standard* CD271 microbeads on MACS MS columns once to enrich for stably transduced cells. To analyze the efficiency of the enrichment process, the three cellular fractions of the MACS separation, the cells after transduction and prior to enrichment (preMACS), the cells not retained by the MACS columns in the magnetic field (flowthrough), and the cells harvested from the columns after removing the magnet (postMACS) were analyzed by flow cytometry for their EGFP expression. Before selection, 60.1% ± 2.6% (N3) and 51.4% ± 11.4% (N4) of the Jurkat cells (Figure 2D, preMACS) and 53.7% ± 1.8% (N3) and 53.9% ± 2.5% (N4) of the T cells (Figure 2E, preMACS) were EGFP positive. The enrichment with the CD271 microbeads on the columns led to highly purified populations: 98.7% ± 0.4% (N3) and 96.6% ± 1.7% (N4) for Jurkat cells (Figure 2D, postMACS) and 98.3% ± 0.5% (N3) and 96.4% ± 2.4% (N4) of the T cells (Figure 2E, postMACS) were transduced/EGFP positive, respectively. However, the enrichment processes were highly inefficient, as the flowthroughs contained 57.2% ± 1.8% (N3) and 49.7% ± 11.7% (N4) EGFP-pos-

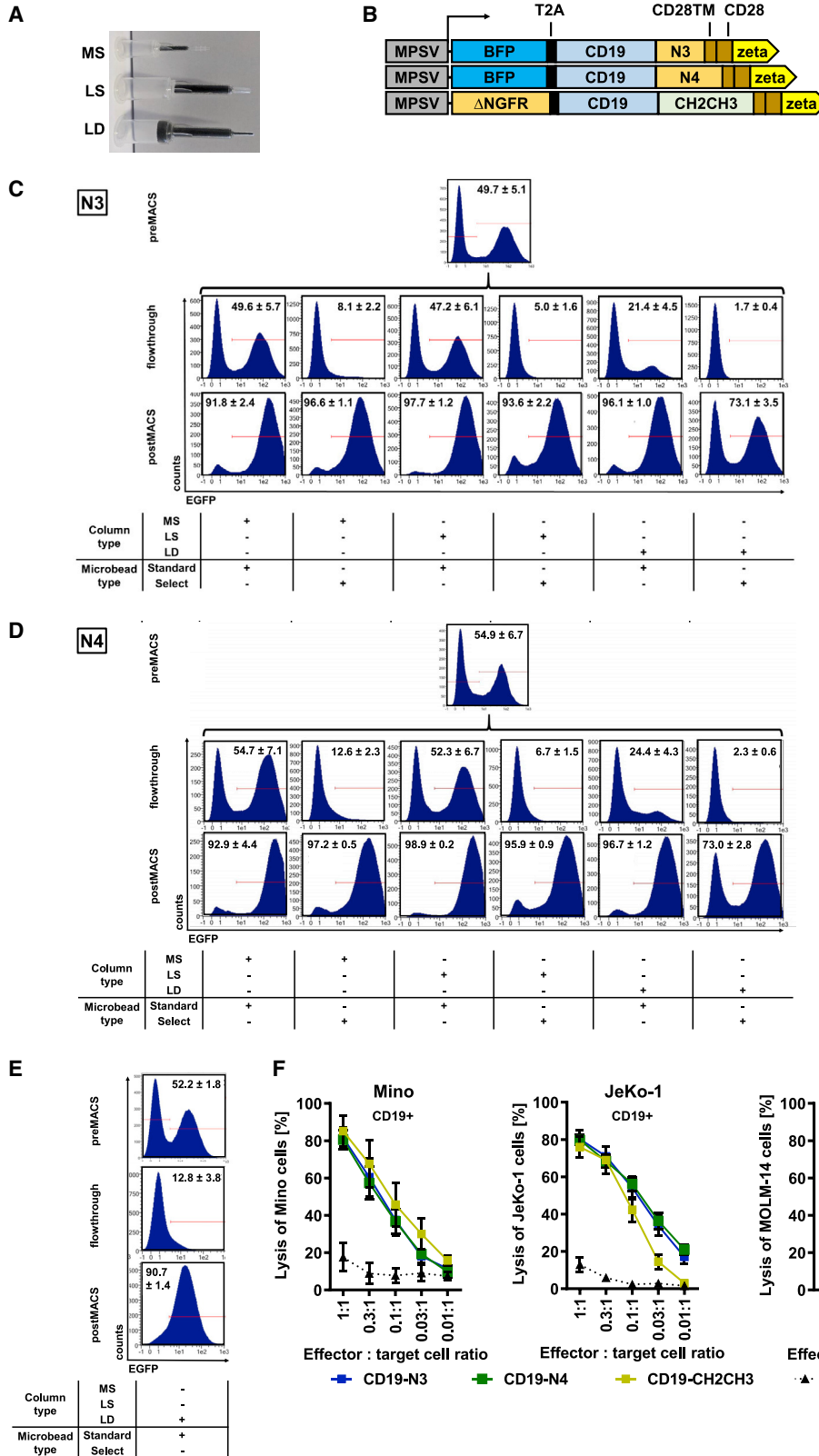
itive Jurkat (Figure 2D, flowthrough) and 50.6% ± 0.8% (N3) and 50.5% ± 2.3% (N4) transduced T cells (Figure 2E, flowthrough), respectively. Thus, before any functional testing, we had to strongly reduce the loss of CAR T cells in the flowthrough of the columns while maintaining pure populations.

Minimizing the loss of CAR T cells on MACS columns

Three different types of column (mini selection [MS], large selection [LS], and large depletion [LD]; Figure 3A), which vary in the length and density of the iron particles, and two different types of CD271 microbead reagents (*Standard*, *Select*), which differ in their antibody-microbead conjugation, are available from Miltenyi Biotec. Thus, we systematically tested whether specific combinations of the column and microbead types (MS + *Standard*, MS + *Select*, LS + *Standard*, LS + *Select*, LD + *Standard*, and LD + *Select*) can be utilized to avoid the high losses of transduced T cells in the flowthrough. To this end, primary human T cells were transduced with bicistronic lentiviral vectors co-expressing EGFP and N3- or N4-hinged CD19 CAR constructs (Figure 3B). Three to 4 days later, the transduced T cells were selected with combinations of three columns and the two CD271 microbead types. Subsequently, samples from preMACS, flowthrough, and postMACS were analyzed by flow cytometry for EGFP expression.

Before enrichment, 49.7% ± 5.1% and 54.9% ± 6.7% of T cells expressed EGFP and hence the N3 or N4 CAR construct, respectively (Figures 3C and 3D; preMACS). All enrichment protocols, except for enrichment with *Select* microbeads in combination with LD columns, led to purities of CAR T cells above 90% (Figures 3C and 3D; postMACS). However, the combination of *Select* microbeads and LD columns resulted in purities of just 73.1% and 73.0%, respectively (Figures 3C and 3D; postMACS). Enrichment with *Standard* microbeads on MS and LS columns also was highly inefficient, since >95% of the CAR T cells were lost in the flowthrough (Figures 3C and 3D; flowthrough). Enrichment with *Standard* microbeads on LD columns was more efficient, since the flowthroughs contained only 21.4% and 24.4% N3- and N4-hinged CD19 CAR T cells, respectively (Figures 3C and 3D; flowthrough). Importantly, the most efficient enrichments were achieved by combining *Select* microbeads with MS or LS columns, thereby reaching purities of 93.6% ± 2.2% to 97.2% ± 0.5% (Figures 3C and 3D; postMACS), while the flowthrough only contained 5.0% ± 1.6% to 12.6% ± 2.3% CAR T cells (Figures 3C and 3D; flowthrough). Since enrichment with *Select* microbeads and MS columns reached a slightly higher purity and the MS magnet enables eight simultaneous separations, in contrast to the LS/LD magnet with a capacity of just four columns, we continued with the MS/*Select* combination for enrichment of N3- and N4-hinged CAR T cells.

ME20.4, or CD19 CAR detection reagent stained with anti-biotin-APC) and EGFP expression. Subsequently, N3- and N4-hinged CAR Jurkat cells (D) or primary human T cells (E) were enriched via magnetic cell sorting (using CD271 microbeads in combination with MS columns) and the three fractions (preMACS, flowthrough, and postMACS) were flow cytometrically analyzed for EGFP expression. In the overlays, the preMACS analysis was depicted as a blue line, the flowthrough as a green line, and the postMACS measurements as a red line. Representative blots were used and data were shown as means ± SEM of at least three biological replicates.



(legend on next page)

N3- and N4-hinged CD19 CARs lyse tumor cells as efficacious as their CH₂CH₃-hinged counterparts

Next, we compared the lytic capabilities of the new N3- and N4-hinged CD19 CARs with the killing mediated by the original CD19 CAR with an IgG1-derived CH₂CH₃ hinge.^{36,43} To this end, primary human T cells were transduced with bicistronic lentiviral vectors co-expressing BFP and CD19-N3 or CD19-N4 or a construct with ΔNGFR and CD19-CH₂CH₃ (Figure 3B). Four days after transduction, N3- and N4-hinged CD19 CAR T cells were enriched with *Select* microbeads on MS columns, while ΔNGFR/CD19-CH₂CH₃ CAR T cells were enriched with *Standard* microbeads on LD columns, which allowed to enrich these cells to purities of 90.7% ± 1.4% (Figure 3E). Co-culturing the three CD19 CAR T cell populations differing in the hinge sequence overnight with EGFP-expressing Mino (CD19⁺) or JeKo-1 (CD19⁺) mantle cell lymphoma (MCL) and MOLM-14 acute monocytic leukemia (AML) (CD19⁻) cells revealed that CD19-N3 and CD19-N4 CAR T cells killed the CD19⁺ Mino and JeKo-1 cells as efficaciously as CD19-CH₂CH₃ CAR T cells (Figure 3F). Importantly, the CD19⁻ MOLM-14 cells were not eliminated by N3- and N4-hinged CD19 CAR T cells, while the CH₂CH₃-hinged CD19 CAR T cells nonspecifically eradicated MOLM-14 cells (Figure 3F). This nonspecific activation of the CH₂CH₃-hinged CAR by MOLM-14 cells is most likely due to the presence of Fcγ receptors on these cells⁴⁴ and was described previously.^{7,24}

N3- and N4-hinged CD19 CARs function comparably to their CD8-hinged counterparts

To establish our NGFR-derived hinges as potential candidates for clinical use, we compared the efficacy of N3- and N4-hinged CD19 and CD33 CAR constructs to counterparts that contained a 48 aa hinge region derived from the human CD8 α-chain.^{45,46} Importantly, this CD8 sequence is used as the hinge in multiple CAR constructs³ including the clinically approved CAR T cell products Kymriah⁴⁶ and Abecma.⁴⁷ To enable enrichment of CD8-hinged CAR T cells with CD271 microbeads, we also included the ΔNGFR cDNA in the vector with the CD8-hinged constructs. Primary human T cells were transduced with bicistronic lentiviral vectors co-expressing BFP and N3- or N4-hinged or ΔNGFR and CD8-hinged CD19 or CD33 CARs (Figure 4A), CAR T cells enriched via MACS and then co-cultured with EGFP-expressing Mino (CD19⁺ CD33⁻), REH (CD19⁺ CD33⁻), or MOLM-14 cells (CD19⁻ CD33⁺). When comparing the expression of the N3- and N4-hinged CARs with the CD8-hinged counterpart using the CD19 CAR detection reagent, we noticed that expression levels of the two NGFR-hinged CARs were

at least comparable with the expression of the CD19-CD8h CAR construct (Figure 4B).

The N3- and N4-hinged CD19 CAR T cells lysed the CD19⁺ cell lines Mino and REH, but not MOLM-14, as efficaciously as the CD19 CAR construct with the CD8 hinge (Figure 4C). Remarkably, the cytokine profiles of the three CD19 CAR T cell products were almost identical when analyzing IFN-γ, GM-CSF, and TNF-α in supernatants of the co-cultures with Mino and REH cells (Figure 4D). It was noteworthy that co-cultures of the CD19 CAR T cells with the MCL Mino cells generally induced higher levels of cytokines compared with co-cultures with B cell precursor ALL REH cells. The CD33 CAR T cells remained nonresponsive against Mino cells, as the lysis remained at background levels (Figure 4C) and no inflammatory cytokines were induced, comparable with the incubation of the cell lines with untransduced T cells (Figure 4D). Co-culture of CD19⁺ CD33⁻ REH cells with N3/N4-hinged CD33 CAR T cells showed no specific lysis and no secretion of cytokines, while the CD8-hinged CD33 CAR T cells minimally lysed REH cells, albeit without induction of cytokines (Figures 4C and 4D). The CD33⁺ CD19⁻ MOLM-14 cells were efficaciously eliminated by all three CD33 CARs and the N3/N4-hinged CARs again proved to be as efficacious as the CD8-hinged CARs (Figure 4C). In the co-cultures with MOLM-14 cells, the CD33 CARs but not the CD19 CARs induced secretion of IFN-γ, GM-CSF, and TNF-α by T cells, comparable with the secretion profiles observed for CD19 CAR T cells upon co-culture with REH cells (Figure 4D).

N3 and N4 hinges can be used as the hinge in different CAR constructs

After establishing that N3- and N4-hinged CD19 and CD33 CAR constructs are as efficacious and specific as their CD8-hinged counterparts, we constructed three additional CARs with scFvs against ROR1, CD5, and CD123 with N3 or N4 hinges and also included the N3- or N4-hinged CD33 CAR constructs as controls in these experiments (Figure 5A). T cells were transduced with bicistronic lentiviral vectors co-expressing BFP and N3- or N4-hinged ROR1, CD5, CD33, or CD123 CARs; CAR T cells were enriched by MACS and co-cultured with EGFP-expressing Mino, JeKo-1, or MOLM-14 cells.

While Mino cells (ROR1⁺, CD5⁺, CD33⁻, CD123⁻) were only partially eliminated by N3-hinged ROR1 and CD5 CAR T cells (Figure 5B), the specific lysis increased when the cells were incubated with the N4-hinged counterparts (Figure 5C). Untransduced as well as CD33 and CD123 CAR T cells did not exhibit any cytotoxicity against

Figure 3. Enrichment of N3- and N4-hinged CD19 CAR T cells can be optimized by applying different microbeads or columns

(A) Photograph of the three columns used. Primary human T cells were lentivirally transduced with constructs co-expressing EGFP in *cis* with CD19-N3, CD19-N4, or CD19-CH₂CH₃ depicted in (B). Three days after transduction CD19-N3 cells (C) or CD19-N4 CAR T cells (D) were enriched with combinations of *Standard* or *Select* microbeads and MS, LS, or LD columns. (E) CD19-CH₂CH₃ CAR T cells were stained with *Standard* microbeads and separated on LD columns. Afterwards, the three fractions (preMACS, flowthrough, and postMACS) were flow cytometrically analyzed for EGFP expression. Representative blots are shown. Values are indicated as percentages and data are depicted as means ± SEM of at least three biological replicates. (F) MACS-enriched CD19-N3, CD19-N4, or CD19-CH₂CH₃ CAR T cells were co-cultured with EGFP-expressing Mino, JeKo-1, or MOLM-14 cells at various effector:target cell ratios. After 16 h co-culture, propidium iodide was added for viable/dead discrimination and samples were analyzed by flow cytometry for lysis of target cells by effector cells. Data were depicted as means ± SEM of at least three biological replicates.

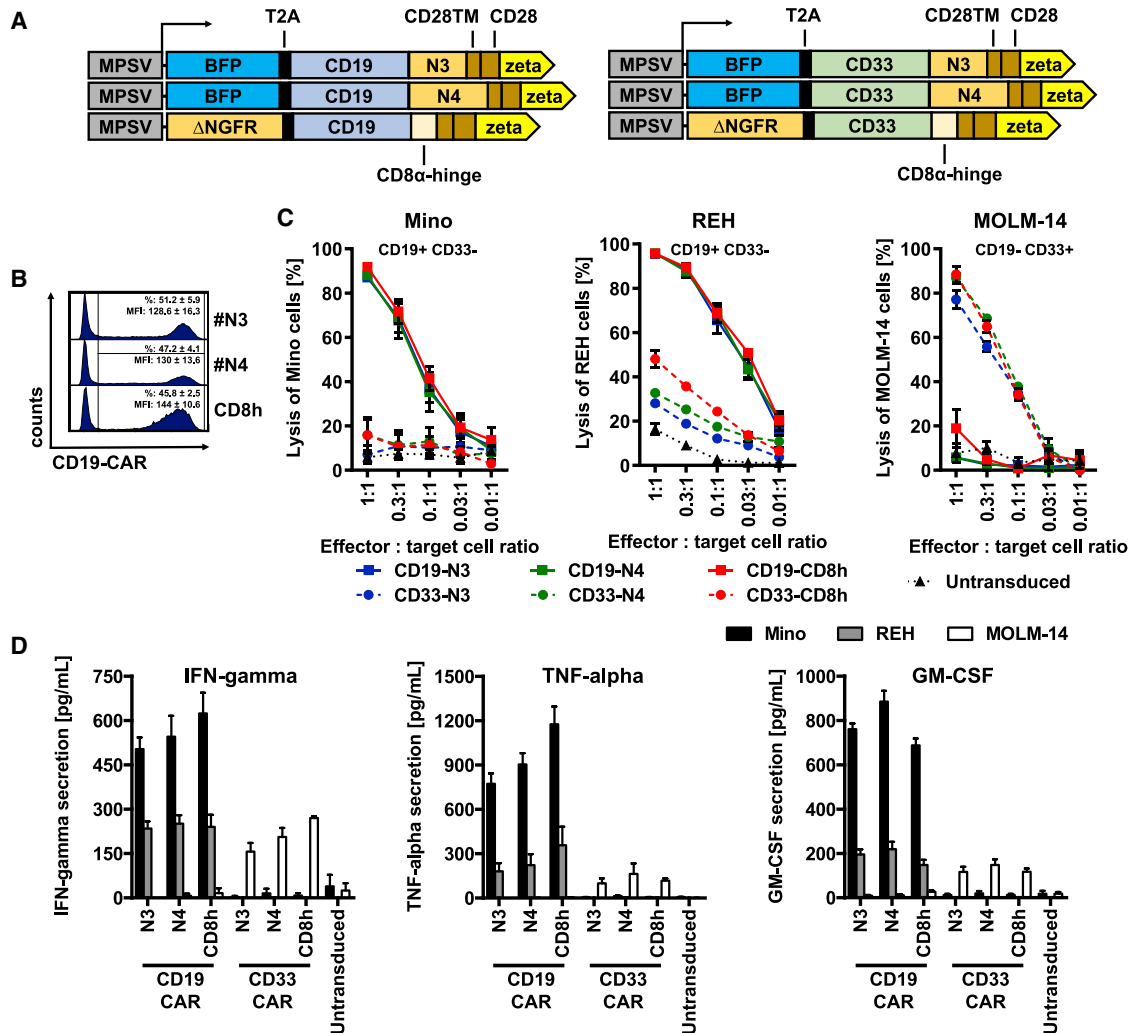


Figure 4. N3- and N4-hinged CD19 and CD33 CARs are as efficacious as CD8-hinged counterparts *in vitro*

Primary human T cells were lentivirally transduced with constructs co-expressing BFP *in cis* with N3- or N4-hinged CD19 or CD33 CARs or Δ NGFR *in cis* with CD8-hinged CD19 or CD33 CARs depicted in (A). (B) Three days after transduction, the T cells were flow cytometrically analyzed for CAR expression (via staining with CD19 CAR detection reagent) and enriched via magnetic cell sorting (CD271 MACSelect microbeads plus MS columns). Subsequently, CAR T cells were co-cultured with EGFP-expressing Mino, REH, or MOLM-14 cells at various effector:target cell ratios. (C) After 16 h co-culture, propidium iodide was added for viable/dead discrimination and samples were analyzed by flow cytometry for lysis of target cells by effector cells. (D) Co-culture supernatants were analyzed for the presence of IFN- γ , GM-CSF, and TNF- α by MACSplex. Data were depicted as means \pm SEM of at least three biological replicates.

Mino cells, regardless of the hinge used in the construct. In contrast, elimination of JeKo-1 cells (ROR1⁺, CD5^{low+}, CD33⁻, CD123⁻) by ROR1-N3 and ROR1-N4 as well as CD5-N3 and CD5-N4 CAR T cells was comparable and not influenced by the hinge length. Noteworthy, the CD5 CAR constructs mediated only limited cytotoxicity, as CD5 is only expressed on a subpopulation of JeKo-1 cells.²⁴ Once again, the CD33 and CD123 CAR T cells with either N3 or N4 hinges remained inert, as both target antigens are not expressed on JeKo-1 cells (Figures 5B and 5C). MOLM-14 cells (ROR1⁻, CD5⁻, CD33⁺, CD123⁺) were efficaciously and specifically eliminated by N3- and N4-hinged CD33 and CD123 CAR T cells, respectively, but not by the CD5 and ROR1 CAR T cells (Figures 5B and 5C). In summary,

using the N3 or N4 sequences as hinge in ROR1, CD5, CD33, and CD123 CAR T cells specifically eliminated antigen-positive cells without causing nonspecific lysis.

N3-, N4-, and CD8-hinged CD33 CAR T cells exert equal control of AML blasts *in vivo*

An important preclinical test for the efficacy and safety of the N3 and N4 hinges in CARs in a more complex model is the *in vivo* leukemia control of N3/N4-hinged CAR T cells compared to the control of CAR T cells with a CD8 hinge, thus allowing to see minimal differences and *off-target* cell toxicity over time. First, we engrafted NSG mice with 3.5×10^6 MOLM-14 cells that had been equipped by a

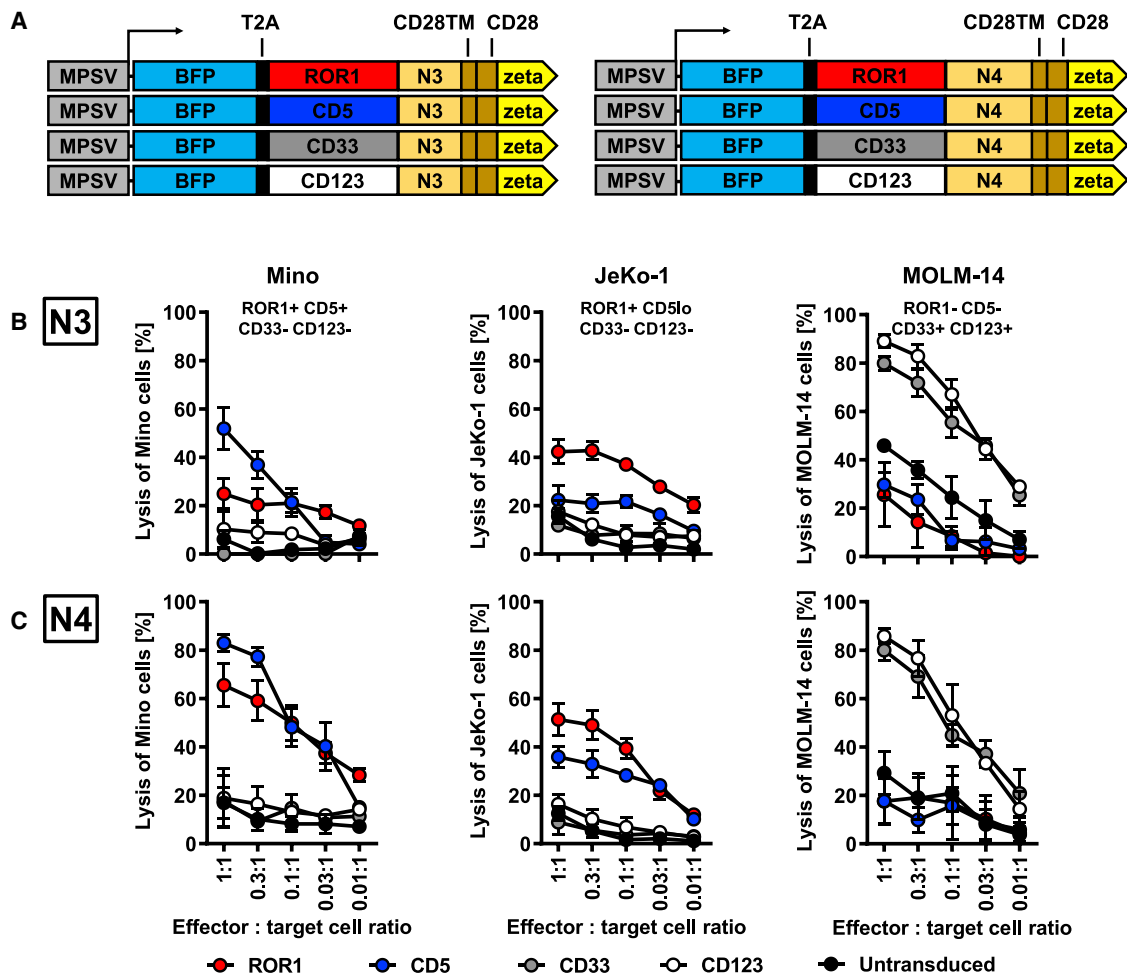


Figure 5. N3- and N4-hinged CARs eliminate malignant cells depending on antigen expression *in vitro*

Primary human T cells were lentivirally transduced with constructs co-expressing BFP in *cis* with N3- or N4-hinged ROR1, CD5, CD33, or CD123 CARs depicted in (A). Three days after transduction, CAR T cells were enriched via magnetic cell sorting (CD271 MACSelect microbeads plus MS columns for all constructs). Subsequently, N3-hinged (B) and N4-hinged (C) CAR T cells were co-cultured with EGFP-transduced Mino, JeKo-1, or MOLM-14 cells at various effector:target cell ratios. After 16 h co-culture, propidium iodide was added for viable/dead discrimination and samples were analyzed flow cytometrically for lysis of target cells by effector cells. Data were depicted as means ± SEM of at least three biological replicates.

lentiviral vector with a luciferase-EGFP fusion gene (LucEG).²⁴ The engraftment of the blasts was assessed 6 days later by luminescence imaging, revealing robust leukemia growth in almost all mice (Figure 6A). We then intravenously administered 3.5×10^6 CD19 or CD33 CAR T cells that contained N3, N4, or CD8 as hinges (Figure 4A) and which had been enriched by MACS to >90% purity. Mice in the control group did not receive a human T cell graft. The persistence of MOLM-14/LucEG cells and CAR T cells was analyzed on days 13, 20, 27, and 34 via luminescence imaging and/or flow cytometry after staining of peripheral blood with directly conjugated antibodies for murine cells (mCD18), human cells (CD45), T cells (CD3), and CAR expression (CD271). The content of AML blasts in the bone marrows was determined by flow cytometry upon sacrifice of the animals.

Untreated NSG mice experienced rapid progression of the AML, as shown by luminescence imaging (Figures 6A and 6B) and blood analysis (Figure 6D), and had to be sacrificed between days 21 and 25 (Figure 6C). The analyses of the animals at sacrifice demonstrated that the bone marrow was strongly infiltrated by MOLM-14/LucEG cells (Figure 6E). Treatment of the animals with CD19 CAR T cells, irrespective of the hinge, did not improve survival, as the disease rapidly progressed also in these animals (Figures 6A–6E). Although CD19 CAR T cells do not recognize MOLM-14 cells (Figure 4B), these CAR T cells still persisted for about three weeks, until sacrifice of the animals, in the bloodstream of the mice (Figure 6F) and could be detected at low levels in the bone marrow at sacrifice (Figure 6G). Importantly, the persistence of CD19 CAR T cells occurred irrespective of the hinge used, and did not influence the leukemia

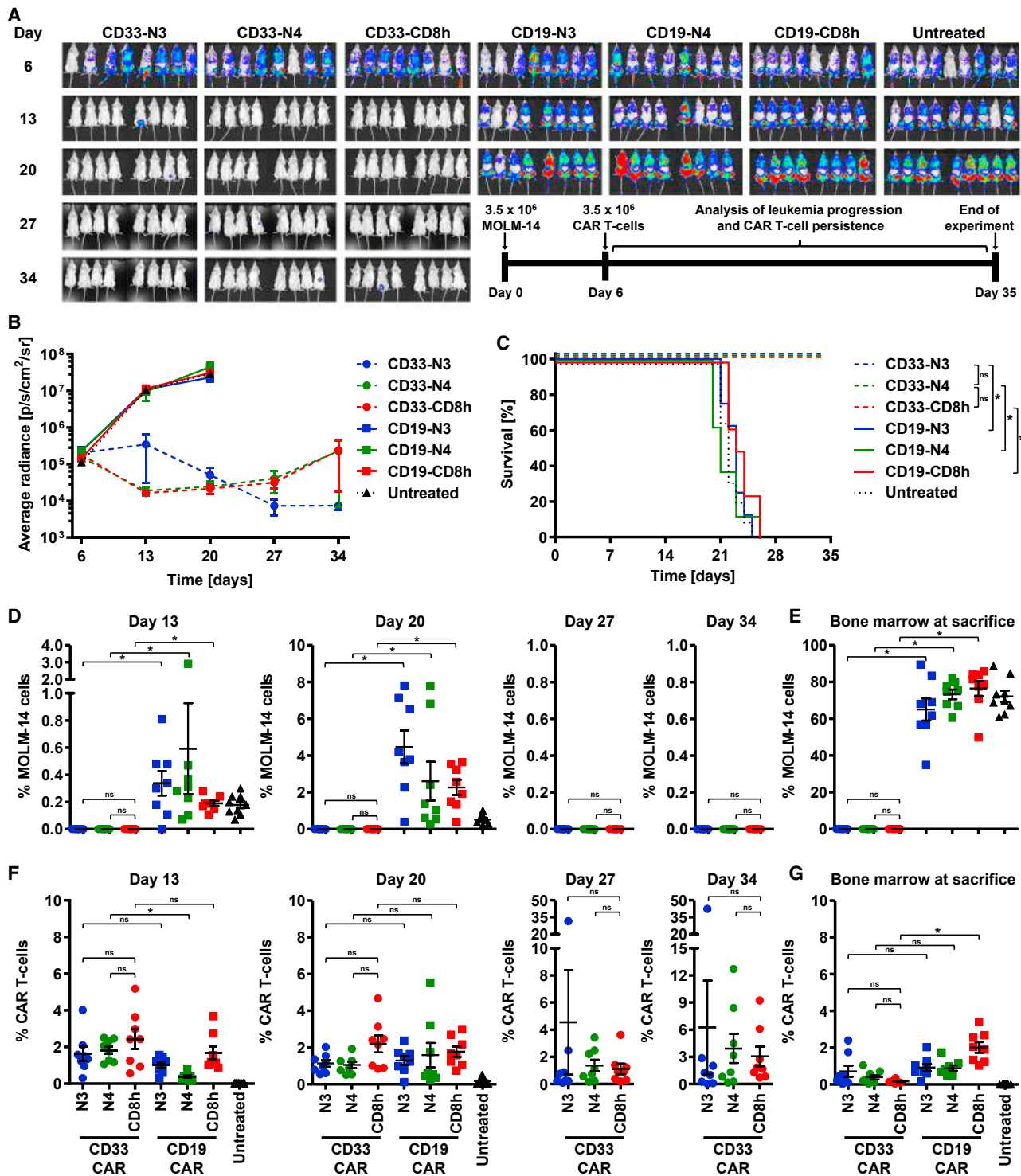


Figure 6. N3- and N4-hinged CD19 and CD33 CARs control AML progression as efficacious as CD8-hinged counterparts

NOD-SCID-gamma mice were xenografted with 3.5×10^6 MOLM-14/LucEG cells. After 6 days, mice were xenografted with a single dose of 3.5×10^6 N3-, N4-, or CD8-hinged CD19 or CD33 CARs or left untreated. To monitor disease progression, luminescence was measured on days 6, 13, 20, 27, and 34 (A and B), blood was flow

(legend continued on next page)

control/survival of the animals. Treatment of the animals by administration of CD33-CAR T cells strongly reduced the leukemia burden and persistence and thus improved the overall survival (Figure 6). Here, it was obvious that N3- and N4-hinged CAR T cells proved to be as efficacious as their CD8-hinged counterparts (Figures 6A–6C). Blood analysis demonstrated that CD33 CAR T cells had engrafted well and persisted in the blood stream for up to 34 days, comparably to the animals that had received CD19 CAR T cells (on days 13 and 20; Figure 6F). Upon sacrifice of the animals, the BM samples of mice in all three CD33 CAR groups were devoid of AML blasts (Figure 6E), despite the previous findings that one to two animals in each group temporarily showed signs of extramedullary disease at single time points (Figure 6A). Finally, we did not observe any toxicity in mice treated with CD8-, N3-, or N4-hinged CAR T cells, suggesting that our NGFR-derived hinges are as efficacious and safe to use as the CD8 hinge.

DISCUSSION

In this work, we developed and validated two human NGFR/CD271-based hinges, N3 and N4, for inclusion in CAR constructs that facilitate both efficient enrichment of the genetically modified CAR T cells using the MACS technology (Miltenyi Biotec) and detection of CAR-positive cells *in vitro* and *in vivo* using staining with directly coupled antibodies and flow cytometry. Although N3 (120 aa) was shorter than N4 (162 aa), both hinges were highly comparable in their MACS enrichment efficiency with *Select* microbeads, their cytotoxicity, and their cytokine induction against leukemia and lymphoma cell lines *in vitro* as well as in their *in vivo* control of AML blasts in NSG mice. However, in CARs against ROR1 and CD5, the N4-hinged counterpart executed slightly higher killing of Mino cells compared with the N3 hinge. Whether this is specific for this cell line or depends on the CAR affinity needs to be evaluated in future studies.

Other groups already used amino acid sequences of the NGFR/CD271 surface domain as selection and detection marker after retroviral gene transfer into hematopoietic stem/progenitor cells as well as T cells.^{38,42} Recently, Casucci et al.¹² included four different amino acid stretches binding the CD271 monoclonal antibody ME20.4 as hinges into a CD44v6 CAR construct: The longest hinge of 222 aa (NWL) contained the complete wild-type surface unit of NGFR, and a second hinge contained all four repeats but without the S/R-rich stalk (NWS). To prevent NGF binding,⁴⁸ they further constructed two hinges (NML and NMS) by introducing mutations in the fourth CRD of NWL and NWS. Importantly, only the NWL hinge with the complete surface unit of NGFR allowed selection of transduced T cells with directly conjugated microbeads, remarkably however this procedure was quite inefficient (yield of ~40%). For the other three hinges, the author even had to use a two-step procedure

with a PE-labeled CD271 antibody followed by anti-PE microbeads,¹² which certainly will be a problem for applications in humans. Although none of the hinges appears satisfactory for the purification process (loss of >50% transduced cells in the flowthrough),¹² a lentiviral vector co-expressing a high-affinity CD44v6 CAR with the NWL hinge and herpes simplex virus 1 thymidine kinase suicide gene³⁹ is currently being employed in a phase I/IIa trial for AML and MM (NCT04097301).

In a more recent publication, the same group reported three new variants of the non-mutated full-length NWL hinge by shortening the S/R-rich stalk.¹⁷ The shortest of these constructs, NWN2, with a length of 173 aa, was functionally almost undistinguishable from the NWL isoform in all assays. Strikingly, however, the CD44v6.NWN2 CAR T cells could also not be efficiently selected with ME20.4-based MACS microbeads; instead, the authors relied once again on a two-step procedure with ME20.4-PE staining followed by sheep-anti-mouse IgG1-coated microbeads, leading to purities of 90%, but yields for NWL and NWN2 CAR T cells of only 40% and 33%, respectively.¹⁷

Our novel NGFR-derived hinges are shorter and more efficient

Our two hinges allowed detecting the expression of CAR constructs on genetically modified T cells from *in vitro* and *in vivo* samples. They also facilitated very efficient and pure enrichment of CAR T cells, which is paramount if the intended use of the hinge is to produce pure CAR T cell products that can be controlled in patients due to co-expression of a suicide gene in the vector. For most CARs recognizing noncritical membrane-distant epitopes, we believe that the N3 hinge with 120 aa will suffice; however, more membrane-proximal located epitope as described for a ROR1 scFv⁶ or CD44v6 isoforms¹⁷ might require a longer hinge, such as N4. Importantly, the specific requirements for the hinge have to be determined for every CAR and targeted epitope on the malignant cells.

Our work here clearly demonstrated that enrichment of transduced cells via MACS needs to be optimized by determining the optimal combination of microbeads and columns. Based on our findings, we suspect that Casucci et al. as well as Stornaiuolo et al.^{12,17} used a nonoptimal MACS protocol, leading to a loss of more than 50% of their CAR T cells on the columns. While the *Select* microbeads appear to be more highly concentrated, which improves retention of the cells within the magnetic field and thus MACS efficiency, the loss of genetically modified CAR T cells in the flowthrough of columns can partly also be avoided by using columns with a higher capacity e.g. the LD columns. However, we currently do not know whether this approach will translate well into the selection protocol used on the CliniMACS or Prodigy devices. In addition, the fact that our NGFR-derived

cytometrically analyzed on days 13, 20, 27, and 34 (D), and bone marrow was flow cytometrically analyzed upon sacrifice of the animals (E). To monitor CAR T cell persistence, blood was flow cytometrically analyzed on days 6, 13, 20, 27, and 34 (F) and bone marrow was flow cytometrically analyzed upon sacrifice of the animals (G). (C) Kaplan-Meier-Survival curves for the seven treatment groups with eight animals per group. p values were calculated by (C) log rank test or (D–G) one-way ANOVA with Dunn's correction for multiple comparisons. The asterisks indicated statistical significance; ns, not significant. Data were depicted as means ± SEM with eight to nine mice per treatment group.

hinges N3 and N4 contain the entire S/R-rich stalk also seems to be important for high-level CAR expression, as Stornaiuolo et al.¹⁷ reported the shortening of the stalk to be associated with larger amounts of CAR constructs remaining in the intracellular compartment. Finally, in contrast to the two previous publications from Casucci et al. and Stornaiuolo et al.,^{12,17} we rigorously demonstrated here that our NGFR-derived hinges are functionally indistinguishably from an already clinically used CD8 hinge in *in vitro* assays and *in vivo* in a xenotransplantation model for AML, but still facilitate efficient recognition and also selection of CAR T cells.

Safety

A hinge cannot only affect CAR function but can also cause unwanted side effects due nonspecific CAR signaling and T cell activation.^{6,7} A well-characterized example of this phenomenon are hinges based on the second and third constant heavy chain domain of human IgG1 or IgG4 (CH₂CH₃). These hinges provide the necessary flexibility, stability, and length for multiple scFvs in CAR constructs to reach their epitopes.^{13,49} However, CH₂CH₃ hinges can also cause *off-target* toxicities by binding to Fc receptors on myeloid cells, thereby mediating activation-induced cell death of the T cells and nonspecific lysis of Fc receptor-positive cells, such as macrophages, monocytes, or NK cells.^{6,7,50} Indeed, as a positive control, we were able to reproduce scFv-independent activation of CH₂CH₃-hinged CAR T cells after co-culture with FcγR expressing MOLM-14 cells.⁴⁴ In contrast, our N3 and N4 hinges were not activated by target antigen-negative cells in any of our experiments *in vitro* and *in vivo*, thus suggesting that no *off-target* effects are mediated by the hinges. Finally, Casucci et al.¹² observed that incubation of NGFR-hinged CAR T cells, containing the entire surface domain of NGFR, with supraphysiological concentrations of NGF, did not affect the transduced cells, probably as important transmembrane and cytoplasmic sequences required for NGF binding and receptor dimerization were missing in these constructs.^{48,51,52}

Two hinges for Split-CAR approaches

We previously reported the development of a CD34-derived hinge with a 99 aa sequence of human CD34,²⁴ which contained the 16 aa epitope of CD34 recognized by the antibody clone QBend-10.⁵³ Thus, we now potentially have two different hinges available for efficient CAR T cell enrichment under GMP-compliant conditions. Individual staining and/or selection procedures enabled by two hinges are important for *Split-CAR* approaches where two CAR constructs need to be present/monitored on the same cell. Here, the classical intracellular signaling domains CD3ζ and CD28 of a second-generation CAR are split upon two distinct CAR constructs, where each scFv targets a different antigen. Consequently, the T cell is only fully activated by co-current CD28 and CD3ζ signaling, when both *Split-CAR* constructs bind their specific antigens on the target cells.⁵⁴ Ideally, this system allows to reduce *on-target* *off-tumor* toxicities associated with the adoptive CAR T cell treatment, as only a pathologic co-expression of two target antigens leads to the full activation of the CAR T cells and therefore killing of the target cells. However, for this approach to work, the expression of the two CARs needs to be

carefully balanced and the expression of the two target antigens on the malignant cells relatively constant.⁵⁴ We currently are focusing our *Split-CAR* work on MCL as a difficult to treat hematological malignant entity in adults and used the two hinges, N3 and CD34, to co-target combinations of CD19, CD5, and ROR1 (Bister et al., unpublished data).

CONCLUSION

In summary, we developed two novel human NGFR-derived hinges of different lengths that allow manufacturing of pure CAR T cell products, using MACS technology to monitor the CAR expression levels on T cells and flow cytometry to detect the presence of transduced T cells in preclinical models and eventually in patients. Despite being slightly larger, the two hinges proved to be as effective as a human CD8-based hinge *in vitro* as well as *in vivo* without any signs of *off-target* toxicities in the tested systems.

MATERIALS AND METHODS

Construct generation

Human NGFR/CD271 (NP_002498.1) truncated after the transmembrane domain at aa position 276 was codon-optimized for human codon usage and synthesized by GeneArt (Thermo Fisher Scientific, Schwerte, Germany). Hinge fragments of different lengths were generated by PCR amplification and inserted into our self-inactivating lentiviral vector expressing a FMC63-based CD19 CAR with a CH₂CH₃ hinge off a viral MPSV U3 promoter.^{24,43,55} We also used a T2A site for expression of two transgenes.³⁶ ΔNGFR-hinged CD19 CARs were inserted behind and EGFP or tagBFP (referred to as BFP) in front of the T2A site.⁵⁶ Moreover, the N3 and N4 hinges were cloned into codon-optimized CARs recognizing the following human target antigen structures: ROR1 (clone R12^{5,57}), CD5 (clone H65^{58,59}), CD33 (clone DRB2⁶⁰), and CD123 (clone 43⁶¹). CAR constructs with a human CD8-derived hinge/without a ΔNGFR-derived hinge were co-expressed with the codon-optimized cytoplasmically truncated NGFR³⁶ to enable enrichment with directly labeled NGFR microbeads.

Cell culture

The acute T cell leukemia cell line Jurkat, the MCL cell lines Mino and JeKo-1, the acute lymphoblastic leukemia (ALL) cell line REH, and the AML cell line MOLM-14 (all purchased from DSMZ, Braunschweig, Germany) were maintained in RPMI-1640 GlutaMAX medium supplemented with 10% fetal bovine serum (FBS), 100 U/mL penicillin, and 100 μg/mL streptomycin (all from Thermo Fisher Scientific). HEK293T cells (DSMZ) were cultured in DMEM GlutaMAX (Thermo Fisher Scientific) supplemented with 10% FBS, 100 U/mL penicillin, and 100 μg/mL streptomycin. Antigen expression profiles of the used cell lines were published previously.²⁴

Primary human T cells were isolated from peripheral blood of healthy donors who gave written and informed consent according to the protocols (no. 4687 and no. 2019-623) approved by the ethics committee of the University Hospital Düsseldorf. Peripheral blood (PB) mononuclear cells were separated via density gradient centrifugation using

Ficoll-Paque Plus (Cytiva Europe, Freiburg, Germany) according to the manufacturer's instructions. To activate and expand T cells, PBMCs were cultured in IMDM (Sigma-Aldrich, Darmstadt, Germany) supplemented with 10% FBS, 100 U/mL penicillin, 100 µg/mL streptomycin, 2 mM L-glutamine (Thermo Fisher Scientific), and 100 U/mL interleukin-2 (IL-2, Proleukin, Novartis, Basel, Switzerland) on anti-human CD3- (Thermo Fisher Scientific) and anti-human CD28-coated (BD Biosciences, Heidelberg, Germany) six-well plates.

All cells were maintained at 5% CO₂, 95% humidity, and 37°C.

Production of lentiviral vectors and transduction of eukaryotic cells

Vesicular stomatitis virus G glycoprotein-pseudotyped replication-deficient lentiviral vectors were generated by polyethyleneimine transfection (Sigma-Aldrich, Darmstadt, Germany) of 6 µg pczVSV-G, 6 µg pCD-NL/BH, and 6 µg vector plasmid into HEK 293T cells as described previously.^{24,62,63} Two days after transfection, virus-containing supernatant was harvested, filtered (0.45 µm), and used for transduction of eukaryotic cells. For the transduction of Jurkat or primary human T cells, 5×10^5 cells were incubated with 2 mL virus-containing supernatant and 10 µg/mL protamine phosphate (Sigma-Aldrich) for 24 h, replenished with fresh medium, and used for experiments after 48 h.

Mino, JeKo-1, REH, or MOLM-14 cells were transduced with limited dilutions of lentiviral vectors to express EGFP and G418 resistance or a firefly luciferase-EGFP fusion protein with subsequent antibiotic selection and/or flow-assisted cell sorting as described previously.^{24,62,64}

Cell enrichment via MACS and flow cytometry

Three to four days after transduction, CAR T cells were enriched with magnetic microbeads and separation columns from Miltenyi Biotec (Bergisch Gladbach, Germany) according to the manufacturer's instructions. In brief, cells were labeled with either CD271 microbeads (from now on referred to as *Standard* microbeads) or LNGFR MAC-Select microbeads (from now on referred to as *Select* microbeads) and separated on MS (maximal capacity: 1×10^7 cells), LS (maximal capacity: 1×10^8 cells), and LD (maximal capacity: 5×10^8 cells) columns. The three fractions (preMACS, flowthrough, and postMACS) were flow cytometrically analyzed on a MACSQuant Analyzer X for EGFP, CAR expression, and ΔNGFR expression via staining with CD271-PE (clone ME20.4, Miltenyi Biotec).

The expression levels of CD19 CAR constructs were determined by flow cytometry using the biotin-coupled CD19 CAR detection reagent followed by staining with anti-biotin-PE or anti-biotin-APC monoclonal antibodies (all reagents from Miltenyi Biotec).

Functional *in vitro* assays

CAR-mediated cytotoxicity of CAR T cells against malignant cell lines was measured via flow cytometry. CAR T cells were co-cultured at various ratios with 2×10^4 EGFP-transduced Mino, JeKo-1, REH,

or MOLM-14 cells for 16 h in U-bottom 96-well plates. Subsequently, supernatants were harvested and frozen at -20°C for cytokine analysis, cells were washed and stained with 1 µg/mL propidium iodide (Sigma-Aldrich) for dead/viable distinction, analyzed on the MACSQuant Analyzer X, and data were evaluated with the MACSQuantify Software 2.11. Tumor cell lysis was determined as 100% - (number of viable tumor cells after co-culture with CAR T cells/number of viable tumor cells without CAR T cells) × 100%. Negative lysis rates were set to be 0%.

Cytokine secretion by CAR T cells was analyzed using the MACSPlex Cytotoxic T/NK cell kit (Miltenyi Biotec) according to the manufacturer's instructions. Per analysis, 50 µL undiluted supernatant was used.

In vivo xenograft model

Animal studies were approved by the state animal research committee (LANUV, NRW, Germany) and all animals were cared for according to the guidelines set by the Federation of European Laboratory Animal Associations. Six- to 8-week-old female NOD.Cg-Prkdc^{SCID}Il2rg^{tm1Wjl}/SzJ (NOD-SCID gamma; NSG) mice (Charles River Laboratories, Sulzfeld, Germany) were intravenously engrafted with 3.5×10^6 MOLM-14 cells stably expressing a firefly luciferase-EGFP fusion protein (LucEG). Six days later, mice were intravenously injected with 3.5×10^6 N3-, N4-, or CD8-hinged CD19 or CD33 CAR T cells. At days 6, 13, 20, 27, and 34, the persistence of MOLM-14 cells was assessed via luminescence imaging and PB analysis. For luminescence imaging, mice were intraperitoneally injected with D-luciferin (OZ Biosciences SAS, Marseilles, France) and after 5 min luminescence was measured in a Caliper IVIS Lumina II system (PerkinElmer LAS, Rodgau, Germany) with an exposure time of 15 s. PB was drawn from the tail vein, the erythrocytes lysed with BD Pharm Lyse (BD Biosciences), and the samples analyzed on a MACSQuant Analyzer X flow cytometer for EGFP, CD33, and CD45 expression for MOLM-14 cells and BFP, CAR (ΔNGFR), CD3, and CD45 expression for CAR T cells after staining with CD271-PE, CD3-PerCP-Vio700, CD45-APC, and CD33-APC-Vio770 (all from Miltenyi Biotec).

Statistical analysis

Statistical analysis was performed with GraphPad Prism 9. p values were calculated using one-way ANOVA with Dunn's correction for multiple comparisons of log rank test. p values below 0.05 were considered statistically significant and are indicated by an asterisk.

ACKNOWLEDGMENTS

We gratefully acknowledge the healthy donors who provided peripheral blood for the *in vitro* and *in vivo* studies. We would like to thank Jörg Schipper, MD, director of the ENT clinic, for his support of this research project. We are also in debt to Wolfgang Schulz, PhD, and Michèle Hoffmann, PhD, both in the Department of Urology, Heinrich Heine University, for the use of the MACSQuant Analyzer X. We acknowledge support by the Open Access Publication Fund of the University of Duisburg-Essen. This work was supported, in part, by

funding from the Medical Research School Düsseldorf, DSO, Heinrich-Heine-Universität Düsseldorf, and the Forschungskommission of the Medical Faculty (KR/27/2016), Heinrich Heine University Dü, the Deutsche Forschungsgemeinschaft (CW/2021-06), the Essener Elterninitiative zur Unterstützung krebskranker Kinder e.V. and within the framework of the iCAN33 project, funded by the European Regional 470 Development Fund NRW (ERDF, German EFRE) 2014–2020.

AUTHOR CONTRIBUTIONS

A.B., T.I., K.R., M.W., K.S., N.G., C.W., and H.H. planned the experiments. A.B., T.I., C.H., G.G., D.S., M.S., and K.R. conducted the experiments. A.B., T.I., M.S., K.R., and G.G. analyzed the data. A.B., C.H., G.G., K.S., C.W., and H.H. wrote the manuscript. All authors approved the final manuscript.

DECLARATION OF INTERESTS

H.H., C.W., T.I., and K.R. are inventors on a patent describing the NGFR hinges. All other authors declare no competing interests.

REFERENCES

- Gross, G., Waks, T., and Eshhar, Z. (1989). Expression of immunoglobulin-T-cell receptor chimeric molecules as functional receptors with antibody-type specificity. *Proc. Natl. Acad. Sci. USA* 86, 10024–10028. <https://doi.org/10.1073/pnas.86.24.10024>.
- June, C.H., and Sadelain, M. (2018). Chimeric antigen receptor therapy. *N. Engl. J. Med.* 379, 64–73. <https://doi.org/10.1056/NEJMr1706169>.
- Larson, R.C., and Maus, M.V. (2021). Recent advances and discoveries in the mechanisms and functions of CAR T cells. *Nat. Rev. Cancer* 21, 145–161. <https://doi.org/10.1038/s41568-020-00323-z>.
- Albinger, N., Hartmann, J., and Ullrich, E. (2021). Current status and perspective of CAR-T and CAR-NK cell therapy trials in Germany. *Gene Ther.* 28, 513–527. <https://doi.org/10.1038/s41434-021-00246-w>.
- Hudecek, M., Lupo-Stanghellini, M.T., Kosasih, P.L., Sommermeyer, D., Jensen, M.C., Rader, C., and Riddell, S.R. (2013). Receptor affinity and extracellular domain modifications affect tumor recognition by ROR1-specific chimeric antigen receptor T cells. *Clin. Cancer Res.* 19, 3153–3164. <https://doi.org/10.1158/1078-0432.CCR-13-0330>.
- Hudecek, M., Sommermeyer, D., Kosasih, P.L., Silva-Benedict, A., Liu, L., Rader, C., Jensen, M.C., and Riddell, S.R. (2015). The nonsignaling extracellular spacer domain of chimeric antigen receptors is decisive for in vivo antitumor activity. *Cancer Immunol. Res.* 3, 125–135. <https://doi.org/10.1158/2326-6066.CIR-14-0127>.
- Hombach, A., Hombach, A.A., Abken, H., and Hombach, A. (2010). Adoptive immunotherapy with genetically engineered T cells: modification of the IgG1 Fc 'spacer' domain in the extracellular moiety of chimeric antigen receptors avoids 'off-target' activation and unintended initiation of an innate immune response. *Gene Ther.* 17, 1206–1213. <https://doi.org/10.1038/gt.2010.91>.
- Alabanza, L., Pegues, M., Geldres, C., Shi, V., Wiltzius, J.J.W., Sievers, S.A., Yang, S.C., and Kochenderfer, J.N. (2017). Function of novel anti-CD19 chimeric antigen receptors with human variable regions is affected by hinge and transmembrane domains. *Mol. Ther.* 25, 2452–2465. <https://doi.org/10.1016/j.ymthe.2017.07.013>.
- Fujiwara, K., Tsunei, A., Kusabuka, H., Ogaki, E., Tachibana, M., and Okada, N. (2020). Hinge and transmembrane domains of chimeric antigen receptor regulate receptor expression and signaling threshold. *Cells* 9. <https://doi.org/10.3390/cells9051182>.
- Qin, L., Lai, Y., Zhao, R., Wei, X., Weng, J., Lai, P., Li, B., Lin, S., Wang, S., Wu, Q., et al. (2017). Incorporation of a hinge domain improves the expansion of chimeric antigen receptor T cells. *J. Hematol. Oncol.* 10, 68. <https://doi.org/10.1186/s13045-017-0437-8>.
- Almäsbaq, H., Walseng, E., Kristian, A., Myhre, M.R., Suso, E.M., Munthe, L.A., Andersen, J.T., Wang, M.Y., Kvalheim, G., Gaudernack, G., et al. (2015). Inclusion of an IgG1-Fc spacer abrogates efficacy of CD19 CAR T cells in a xenograft mouse model. *Gene Ther.* 22, 391–403. <https://doi.org/10.1038/mt.2015.4>.
- Casucci, M., Falcone, L., Camisa, B., Norelli, M., Porcellini, S., Stornaiuolo, A., Ciceri, F., Traversari, C., Bordignon, C., Bonini, C., and Bondanza, A. (2018). Extracellular NGFR spacers allow efficient tracking and enrichment of fully functional CAR-T cells Co-expressing a suicide gene. *Front. Immunol.* 9, 507. <https://doi.org/10.3389/fimmu.2018.00507>.
- Guest, R.D., Hawkins, R.E., Kirillova, N., Cheadle, E.J., Arnold, J., O'Neill, A., Irlam, J., Chester, K.A., Kemshead, J.T., Shaw, D.M., et al. (2005). The role of extracellular spacer regions in the optimal design of chimeric immune receptors: evaluation of four different scFvs and antigens. *J. Immunother.* 28, 203–211. <https://doi.org/10.1097/01.cji.0000161397.96582.59>.
- Jonnalagadda, M., Mardiros, A., Urak, R., Wang, X., Hoffman, L.J., Bernanke, A., Chang, W.C., Bretzlaff, W., Starr, R., Priceman, S., et al. (2015). Chimeric antigen receptors with mutated IgG4 Fc spacer avoid fc receptor binding and improve T cell persistence and antitumor efficacy. *Mol. Ther.* 23, 757–768. <https://doi.org/10.1038/mt.2014.208>.
- Koristka, S., Ziller-Walter, P., Bergmann, R., Arndt, C., Feldmann, A., Kegler, A., Cartellieri, M., Ehninger, A., Ehninger, G., Bornhäuser, M., and Bachmann, M.P. (2019). Anti-CAR-engineered T cells for epitope-based elimination of autologous CAR T cells. *Cancer Immunol. Immunother.* 68, 1401–1415. <https://doi.org/10.1007/s00262-019-02376-y>.
- Liu, L., Sommermeyer, D., Cabanov, A., Kosasih, P., Hill, T., and Riddell, S.R. (2016). Inclusion of Strep-tag II in design of antigen receptors for T-cell immunotherapy. *Nat. Biotechnol.* 34, 430–434. <https://doi.org/10.1038/nbt.3461>.
- Stornaiuolo, A., Valentini, B., Sirini, C., Scavullo, C., Asperti, C., Zhou, D., Martinez De La Torre, Y., Corna, S., Casucci, M., Porcellini, S., and Traversari, C. (2021). Characterization and functional analysis of CD44v6.CAR T cells endowed with a new low-affinity nerve growth factor receptor-based spacer. *Hum. Gene Ther.* 32, 744–760. <https://doi.org/10.1089/hum.2020.216>.
- Watanabe, N., Bajgain, P., Sukumaran, S., Ansari, S., Heslop, H.E., Rooney, C.M., Brenner, M.K., Leen, A.M., and Vera, J.F. (2016). Fine-tuning the CAR spacer improves T-cell potency. *Oncoimmunology* 5, e1253656. <https://doi.org/10.1080/2162402X.2016.1253656>.
- Locke, F.L., Ghobadi, A., Jacobson, C.A., Miklos, D.B., Lekakis, L.J., Oluwole, O.O., Lin, Y., Braunschweig, I., Hill, B.T., Timmerman, J.M., et al. (2019). Long-term safety and activity of axicabtagene ciloleucel in refractory large B-cell lymphoma (ZUMA-1): a single-arm, multicentre, phase 1-2 trial. *Lancet Oncol.* 20, 31–42. [https://doi.org/10.1016/S1470-2045\(18\)30864-7](https://doi.org/10.1016/S1470-2045(18)30864-7).
- Cheng, Z., Wei, R., Ma, Q., Shi, L., He, F., Shi, Z., Jin, T., Xie, R., Wei, B., Chen, J., et al. (2018). In vivo expansion and antitumor activity of coinfused CD28- and 4-1BB-engineered CAR-T cells in patients with B cell leukemia. *Mol. Ther.* 26, 976–985. <https://doi.org/10.1016/j.ymthe.2018.01.022>.
- Vairy, S., Lopes Garcia, J., Teira, P., and Bittencourt, H. (2018). CTL019 (tisagenlecleucel): CAR-T therapy for relapsed and refractory B-cell acute lymphoblastic leukemia. *Drug Des. Devel Ther.* 12, 3885–3898. <https://doi.org/10.2147/DDDT.S138765>.
- Smith-Garvin, J.E., Koretzky, G.A., and Jordan, M.S. (2009). T cell activation. *Annu. Rev. Immunol.* 27, 591–619. <https://doi.org/10.1146/annurev.immunol.021908.132706>.
- Valton, J., Guyot, V., Boldajipour, B., Sommer, C., Pertel, T., Juillerat, A., Duclert, A., Sasu, B.J., Duchateau, P., and Poirot, L. (2018). A versatile safeguard for chimeric antigen receptor T-cell immunotherapies. *Sci. Rep.* 8, 8972. <https://doi.org/10.1038/s41598-018-27264-w>.
- Bister, A., Ibach, T., Haist, C., Smorra, D., Roellecke, K., Wagenmann, M., Scheckenbach, K., Gattermann, N., Wiek, C., and Hanenberg, H. (2021). A novel CD34-derived hinge for rapid and efficient detection and enrichment of CAR T cells. *Mol. Ther. Oncolytics* 23, 534–546. <https://doi.org/10.1016/j.omto.2021.11.003>.
- Jena, B., Maiti, S., Huls, H., Singh, H., Lee, D.A., Champlin, R.E., and Cooper, L.J.N. (2013). Chimeric antigen receptor (CAR)-specific monoclonal antibody to detect CD19-specific T cells in clinical trials. *PLoS One* 8, e57838. <https://doi.org/10.1371/journal.pone.0057838>.

26. Lee, D.W., Kochenderfer, J.N., Stetler-Stevenson, M., Cui, Y.K., Delbrook, C., Feldman, S.A., Fry, T.J., Orentas, R., Sabatino, M., Shah, N.N., et al. (2015). T cells expressing CD19 chimeric antigen receptors for acute lymphoblastic leukaemia in children and young adults: a phase 1 dose-escalation trial. *Lancet* 385, 517–528. [https://doi.org/10.1016/S0140-6736\(14\)61403-3](https://doi.org/10.1016/S0140-6736(14)61403-3).
27. Badbaran, A., Berger, C., Riecken, K., Kruchen, A., Geffken, M., Müller, I., Kröger, N., Ayuk, F.A., and Fehse, B. (2020). Accurate in-vivo quantification of CD19 CAR-T cells after treatment with axicabtagene ciloleucel (Axi-Cel) and tisagenlecleucel (Tisa-Cel) using digital PCR. *Cancers* 12, 1970. <https://doi.org/10.3390/cancers12071970>.
28. Ayuk, F., Fehse, B., Janson, D., Berger, C., Riecken, K., and Kröger, N. (2020). Excellent proliferation and persistence of allogeneic donor-derived 41-BB based CAR-T cells despite immunosuppression with cyclosporine A. *Haematologica* 105, E322–E324. <https://doi.org/10.3324/haematol.2019.245969>.
29. Abramson, J.S., Palomba, M.L., Gordon, L.L., Lunning, M.A., Wang, M., Arnason, J., Mehta, A., Purev, E., Maloney, D.G., Andreadis, C., et al. (2020). Lisocabtagene marelucel for patients with relapsed or refractory large B-cell lymphomas (TRANSCEND NHL 001): a multicentre seamless design study. *Lancet* 396, 839–852. [https://doi.org/10.1016/S0140-6736\(20\)31366-0](https://doi.org/10.1016/S0140-6736(20)31366-0).
30. Turtle, C.J., Hanafi, L.A., Berger, C., Gooley, T.A., Cherian, S., Hudecek, M., Sommermeyer, D., Melville, K., Pender, B., Budiarto, T.M., et al. (2016). CD19 CAR-T cells of defined CD4+CD8+ composition in adult B cell ALL patients. *J. Clin. Invest.* 126, 2123–2138. <https://doi.org/10.1172/JCI85309>.
31. Porter, D.L., Hwang, W.T., Frey, N.V., Lacey, S.F., Shaw, P.A., Loren, A.W., Bagg, A., Marcucci, K.T., Shen, A., Gonzalez, V., et al. (2015). Chimeric antigen receptor T cells persist and induce sustained remissions in relapsed refractory chronic lymphocytic leukemia. *Sci. Transl. Med.* 7, 303ra139. <https://doi.org/10.1126/scitranslmed.aac5415>.
32. Maude, S.L., Frey, N., Shaw, P.A., Aplenc, R., Barrett, D.M., Bunin, N.J., Chew, A., Gonzalez, V.E., Zheng, Z., Lacey, S.F., et al. (2014). Chimeric antigen receptor T cells for sustained remissions in leukemia. *N. Engl. J. Med.* 371, 1507–1517. <https://doi.org/10.1056/NEJMoa1407222>.
33. Ritchie, D.S., Neeson, P.J., Khot, A., Peinert, S., Tai, T., Tainton, K., Chen, K., Shin, M., Wall, D.M., Hönemann, D., et al. (2013). Persistence and efficacy of second generation CAR T cell against the LeY antigen in acute myeloid leukemia. *Mol. Ther.* 21, 2122–2129. <https://doi.org/10.1038/mt.2013.154>.
34. Zhang, Q., Hu, H., Chen, S.Y., Liu, C.J., Hu, F.F., Yu, J.M., Wu, Y.H., and Guo, A.Y. (2019). Transcriptome and regulatory network analyses of CD19-CAR-T immunotherapy for B-all. *Genom Proteom Bioinf* 17, 190–200. <https://doi.org/10.1016/j.gpb.2018.12.008>.
35. Canté-Barrett, K., Mendes, R.D., Smits, W.K., van Helsdingen-van Wijk, Y.M., Pieters, R., and Meijerink, J.P.P. (2016). Lentiviral gene transfer into human and murine hematopoietic stem cells: size matters. *BMC Res. Notes* 9, 312. <https://doi.org/10.1186/s13104-016-2118-z>.
36. Roelcke, K., Virts, E.L., Einholz, R., Edson, K.Z., Altwater, B., Rossig, C., von Laer, D., Scheckenbach, K., Wagenmann, M., Reinhardt, D., et al. (2016). Optimized human CYP4B1 in combination with the alkylator prodrug 4-ipomeanol serves as a novel suicide gene system for adoptive T-cell therapies. *Gene Ther.* 23, 615–626. <https://doi.org/10.1038/gt.2016.38>.
37. Johnson, D., Lanahan, A., Buck, C.R., Sehgal, A., Morgan, C., Mercer, E., Bothwell, M., and Chao, M. (1986). Expression and structure of the human NGF receptor. *Cell* 47, 545–554. [https://doi.org/10.1016/0092-8674\(86\)90619-7](https://doi.org/10.1016/0092-8674(86)90619-7).
38. Ciceri, F., Bonini, C., Stanghellini, M.T.L., Bondanza, A., Traversari, C., Salomoni, M., Turchetto, L., Colombi, S., Bernardi, M., Peccatori, J., et al. (2009). Infusion of suicide-gene-engineered donor lymphocytes after family haploidentical haemopoietic stem-cell transplantation for leukaemia (the TK007 trial): a non-randomised phase I-II study. *Lancet Oncol.* 10, 489–500. [https://doi.org/10.1016/S1470-2045\(09\)70074-9](https://doi.org/10.1016/S1470-2045(09)70074-9).
39. Bonini, C., Ferrari, G., Verzeletti, S., Servida, P., Zappone, E., Ruggieri, L., Ponzone, M., Rossini, S., Mavilio, F., Traversari, C., and Bordignon, C. (1997). HSV-TK gene transfer into donor lymphocytes for control of allogeneic graft-versus-leukemia. *Science* 276, 1719–1724. <https://doi.org/10.1126/science.276.5319.1719>.
40. Amaria, R.N., Haymaker, C.L., Bernatchez, C., Forget, M.-A., Patel, V., Hwu, W.-J., Davies, M.A., Patel, S.P., Diab, A., Glitza, I.C., et al. (2016). A phase I/II study of lymphodepletion plus adoptive cell transfer (ACT) with T cells transduced with CXCR2 and NGFR followed by high dose interleukin-2 (IL-2) in patients with metastatic melanoma (MM). *J. Clin. Oncol.* 34, TPS9594. https://doi.org/10.1200/JCO.2016.34.15_suppl.TPS9594.
41. Li, Z., Dullmann, J., Schiedlmeier, B., Schmidt, M., von Kalle, C., Meyer, J., Forster, M., Stocking, C., Wahlers, A., Frank, O., et al. (2002). Murine leukemia induced by retroviral gene marking. *Science* 296, 497. <https://doi.org/10.1126/science.1068893>.
42. Bonini, C., Grez, M., Traversari, C., Ciceri, F., Markt, S., Ferrari, G., Dinauer, M., Sadat, M., Aiuti, A., Deola, S., et al. (2003). Safety of retroviral gene marking with a truncated NGF receptor. *Nat. Med.* 9, 367–369. <https://doi.org/10.1038/nm0403-367>.
43. Landmeier, S., Altwater, B., Pscherer, S., Meltzer, J., Sebire, N., Pule, M., Vera, J., Hotfilder, M., Juergens, H., Vormoor, J., and Rossig, C. (2010). Cytotoxic T cells transduced with chimeric anti-CD19 receptors prevent engraftment of primary lymphoblastic leukemia in vivo. *Leukemia* 24, 1080–1084. <https://doi.org/10.1038/leu.2010.38>.
44. Matsuo, Y., MacLeod, R.A., Uphoff, C.C., Drexler, H.G., Nishizaki, C., Katayama, Y., Kimura, G., Fujii, N., Omoto, E., Harada, M., and Orita, K. (1997). Two acute monocytic leukemia (AML-M5a) cell lines (MOLM-13 and MOLM-14) with interclonal phenotypic heterogeneity showing MLL-AF9 fusion resulting from an occult chromosome insertion, ins(11;9)(q23;p22p23). *Leukemia* 11, 1469–1477. <https://doi.org/10.1038/sj.leu.2400768>.
45. Milone, M.C., Fish, J.D., Carpenito, C., Carroll, R.G., Binder, G.K., Teachey, D., Samanta, M., Lakkhal, M., Gloss, B., Danet-Desnoyers, G., et al. (2009). Chimeric receptors containing CD137 signal transduction domains mediate enhanced survival of T cells and increased antileukemic efficacy in vivo. *Mol. Ther.* 17, 1453–1464. <https://doi.org/10.1038/mt.2009.83>.
46. Schuster, S.J., Bishop, M.R., Tam, C.S., Waller, E.K., Borchmann, P., McGuirk, J.P., Jäger, U., Jaglowski, S., Andreadis, C., Westin, J.R., et al. (2019). Tisagenlecleucel in adult relapsed or refractory diffuse large B-cell lymphoma. *N. Engl. J. Med.* 380, 45–56. <https://doi.org/10.1056/NEJMoa1804980>.
47. Munshi, N.C., Anderson, L.D., Jr., Shah, N., Madduri, D., Berdeja, J., Lonial, S., Raju, N., Lin, Y., Siegel, D., Oriol, A., et al. (2021). Idecabtagene vicleucel in relapsed and refractory multiple myeloma. *N. Engl. J. Med.* 384, 705–716. <https://doi.org/10.1056/NEJMoa2024850>.
48. Yan, H., and Chao, M.V. (1991). Disruption of cysteine-rich repeats of the p75 nerve growth factor receptor leads to loss of ligand binding. *J. Biol. Chem.* 266, 12099–12104. [https://doi.org/10.1016/s0021-9258\(18\)99070-8](https://doi.org/10.1016/s0021-9258(18)99070-8).
49. Moritz, D., and Groner, B. (1995). A spacer region between the single chain antibody and the CD3 zeta-chain domain of chimeric T cell receptor components is required for efficient ligand binding and signaling activity. *Gene Ther.* 2, 539–546.
50. Ravetch, J.V., and Bolland, S. (2001). IgG fc receptors. *Annu. Rev. Immunol.* 19, 275–290. <https://doi.org/10.1146/annurev.immunol.19.1.275>.
51. Shamovsky, I.L., Ross, G.M., Riopelle, R.J., and Weaver, D.F. (2008). The interaction of neurotrophins with the p75NTR common neurotrophin receptor: a comprehensive molecular modeling study. *Protein Sci.* 8, 2223–2233. <https://doi.org/10.1110/ps.8.11.2223>.
52. Vilar, M., Charalampopoulos, I., Kenchappa, R.S., Simi, A., Karaca, E., Reversi, A., Choi, S., Bothwell, M., Mingarro, I., Friedman, W.J., et al. (2009). Activation of the p75 neurotrophin receptor through conformational rearrangement of disulphide-linked receptor dimers. *Neuron* 62, 72–83. <https://doi.org/10.1016/j.neuron.2009.02.020>.
53. Philip, B., Kokalaki, E., Mekkaoui, L., Thomas, S., Straathof, K., Flutter, B., Marin, V., Marafioti, T., Chakraverty, R., Linch, D., et al. (2014). A highly compact epitope-based marker/suicide gene for easier and safer T-cell therapy. *Blood* 124, 1277–1287. <https://doi.org/10.1182/blood-2014-01-545020>.
54. Kloss, C.C., Condomines, M., Cartellieri, M., Bachmann, M., and Sadelain, M. (2013). Combinatorial antigen recognition with balanced signaling promotes selective tumor eradication by engineered T cells. *Nat. Biotechnol.* 31, 71–75. <https://doi.org/10.1038/nbt.2459>.
55. Rössig, C., Pscherer, S., Landmeier, S., Altwater, B., Jürgens, H., and Vormoor, J. (2005). Adoptive cellular immunotherapy with CD19-specific T cells. *Klin Padiatr.* 217, 351–356. <https://doi.org/10.1055/s-2005-872521>.

56. Haist, C., Schulte, E., Bartels, N., Bister, A., Poschinski, Z., Ibach, T.C., Geipel, K., Wiek, C., Wagenmann, M., Monzel, C., et al. (2021). CD44v6-targeted CAR T-cells specifically eliminate CD44 isoform 6 expressing head/neck squamous cell carcinoma cells. *Oral Oncol.* 116, 105259. <https://doi.org/10.1016/j.oraloncology.2021.105259>.
57. Yang, J., Baskar, S., Kwong, K.Y., Kennedy, M.G., Wiestner, A., and Rader, C. (2011). Therapeutic potential and challenges of targeting receptor tyrosine kinase ROR1 with monoclonal antibodies in B-cell malignancies. *PLoS One* 6, e21018. <https://doi.org/10.1371/journal.pone.0021018>.
58. Studnicka, G.M., Soares, S., Better, M., Williams, R.E., Nadell, R., and Horwitz, A.H. (1994). Human-engineered monoclonal antibodies retain full specific binding activity by preserving non-CDR complementarity-modulating residues. *Protein Eng.* 7, 805–814. <https://doi.org/10.1093/protein/7.6.805>.
59. Mamonkin, M., Rouce, R.H., Tashiro, H., and Brenner, M.K. (2015). A T-cell-directed chimeric antigen receptor for the selective treatment of T-cell malignancies. *Blood* 126, 983–992. <https://doi.org/10.1182/blood-2015-02-629527>.
60. Stamova, S., Cartellieri, M., Feldmann, A., Arndt, C., Koristka, S., Bartsch, H., Bippes, C.C., Wehner, R., Schmitz, M., von Bonin, M., et al. (2011). Unexpected recombinations in single chain bispecific anti-CD3-anti-CD33 antibodies can be avoided by a novel linker module. *Mol. Immunol.* 49, 474–482. <https://doi.org/10.1016/j.molimm.2011.09.019>.
61. Stein, C., Kellner, C., Kügler, M., Reiff, N., Mentz, K., Schwenkert, M., Stockmeyer, B., Mackensen, A., and Fey, G.H. (2010). Novel conjugates of single-chain Fv antibody fragments specific for stem cell antigen CD123 mediate potent death of acute myeloid leukaemia cells. *Br. J. Haematol.* 148, 879–889. <https://doi.org/10.1111/j.1365-2141.2009.08033.x>.
62. Wiek, C., Schmidt, E.M., Roellecke, K., Freund, M., Nakano, M., Kelly, E.J., Kaisers, W., Yarov-Yarovoy, V., Kramm, C.M., Rettie, A.E., and Hanenberg, H. (2015). Identification of amino acid determinants in CYP4B1 for optimal catalytic processing of 4-ipomeanol. *Biochem. J.* 465, 103–114. <https://doi.org/10.1042/BJ20140813>.
63. Grunewald, C.M., Haist, C., König, C., Petzsch, P., Bister, A., Nößner, E., Wiek, C., Scheckenbach, K., Köhrer, K., Niegisch, G., et al. (2021). Epigenetic priming of bladder cancer cells with decitabine increases cytotoxicity of human EGFR and CD44v6 CAR engineered T-cells. *Front. Immunol.* 12, 782448. <https://doi.org/10.3389/fimmu.2021.782448>.
64. Gu, D., Liu, H., Su, G.H., Zhang, X., Chin-Sinex, H., Hanenberg, H., Mendonca, M.S., Shannon, H.E., Chiorean, E.G., and Xie, J. (2013). Combining hedgehog signaling inhibition with focal irradiation on reduction of pancreatic cancer metastasis. *Mol. Cancer Ther.* 12, 1038–1048. <https://doi.org/10.1158/1535-7163.MCT-12-1030>.